

Geophysical Research Letters



RESEARCH LETTER

10.1029/2019GL082685

Key Points:

- Optimum multiparameter analysis is used to quantify source water contributions and spatiotemporal variability of water mass structure in the California Current
- Interannual variability in source water mass distributions is associated with regional biogeochemical variability
- ENSO cycle impacts relative contributions and depth structure of source waters, with implications for ecosystem structure

Supporting Information:

Supporting Information S1

Correspondence to:

S. J. Bograd, steven.bograd@noaa.gov

Bograd, S. I., Schroeder, I. D., & Jacox, M. G. (2019). A Water Mass History of the Southern California Current System. Geophysical Research Letters, 46. https://doi.org/10.1029/ 2019GL082685

Received 5 MAR 2019 Accepted 6 MAY 2019 Accepted article online 9 MAY 2019

©2019. The Authors.

This is an open access article under the terms of the Creative Commons Attribution-NonCommercial-NoDerivs License, which permits use and distribution in any medium, provided the original work is properly cited, the use is non-commercial and no modifications or adaptations are made.

A water mass history of the Southern California current system

Steven J. Bograd^{1,2}, Isaac D. Schroeder², and Michael G. Jacox^{1,3}



¹NOAA, Southwest Fisheries Science Center, Environmental Research Division, Monterey, CA, USA, ²Institute of Marine Sciences, University of California, Santa Cruz, Santa Cruz, CA, USA, 3NOAA, Earth System Research Laboratory, Physical Sciences Division, Boulder, CO, USA

Abstract The California Current System represents a confluence of different water masses originating in the subarctic, subtropical, and tropical eastern Pacific. Variations in their relative influence can alter regional biogeochemistry and ecosystem structure. We perform an optimum multiparameter analysis on historical hydrographic data to quantify the spatiotemporal variability of water mass contributions to the California Current. Within the pycnocline, a strong cross-shore gradient in the primary water mass source reflects the dominant advective pathways within the California Current and California Undercurrent. The El Niño Southern Oscillation imparts variability in the relative contributions and depth structure of source waters, allowing stronger upwelling during La Niña to more effectively tap nutrient-rich, oxygen-poor waters originating in the eastern tropical North Pacific. This regional water mass history provides context for understanding the drivers and pathways of biogeochemical variability in the California Current and demonstrates that oceanic changes occurring far afield can have regionally heterogeneous impacts.

Plain Language Summary Waters found in the California Current come from different parts of the ocean: the subarctic, subtropical, and tropical eastern Pacific. Each of these source waters has its own characteristic combination of properties like temperature, saltiness, and nutrient and oxygen levels. Variations in the relative contributions of these source waters can impact local conditions, including oxygen and nutrient content and the properties of upwelled waters. Here we explore long time series of hydrographic data from an oceanic region off southern California to quantify the relative contributions of different source water masses, and their spatial and interannual variability. We describe a spatially heterogeneous water mass structure which is significantly impacted by the El Niño-Southern Oscillation, with important implications for regional biogeochemistry and ecosystem structure. The analysis demonstrates that regional variability in the California Current can be driven by oceanic changes occurring far afield.

1. Introduction

The California Current System (CCS) is a highly productive coastal upwelling biome that is strongly influenced by remote and local physical forcing (M. Jacox et al., 2015; Bograd et al., 2015). Waters within the CCS represent a confluence of different water masses originating in the subarctic, subtropical and tropical eastern Pacific, each with different characteristic properties (Thomson & Krassovski, 2010; Tomczak & Godfrey, 2003). Changes in the relative influence of these water masses can dramatically alter ecosystem structure, as was observed in summer 2002 when anomalously cool, fresh, high-nutrient waters of subarctic origin impacted the CCS and drove exceptionally high primary production (Huyer, 2003). Changes in the relative proportions of water masses has also been implicated in long-term variations of fish community composition in the CCS (McClatchie et al., 2018; Schroeder et al., 2018).

The CCS has also experienced significant biogeochemical trends in recent years that may reflect source water changes. Significant declines in dissolved oxygen (Bograd et al., 2008; McClatchie et al., 2010; Meinvielle & Johnson, 2013; Nam et al., 2015) and concomitant increases in inorganic nutrient content (Bograd et al., 2015) have been observed at the southern end of the system, which are consistent with trends observed throughout the eastern tropical and North Pacific (Chan et al., 2008; Deutsch et al., 2005, 2011; Stramma et al., 2008, 2010; Watanabe et al., 2008; Whitney et al., 2007, 2013). Ocean deoxygenation is an anticipated effect of climate change, as warmer waters reduce oxygen solubility, increase water column stratification, and limit open ocean ventilation (Breitburg et al., 2018; Doney et al., 2009; Gruber, 2011;



Keeling et al., 2010; Levin, 2018). On a global scale, it has been estimated that the world's oceans have lost approximately 2% of their oxygen inventory since 1960 (Schmidtko et al., 2017), although there are large regional differences in rates of loss (Levin, 2018). Climate models project continued deoxygenation trends through the 21st century (Andrews et al., 2017; Bopp et al., 2017), with attendant changes in microbial respiration, increased ocean acidification (Gruber et al., 2012; Hauri et al., 2009), and impacts on biological production, biodiversity, and ecosystem services (Breitburg et al., 2018; Koslow et al., 2018; Levin, 2018; Limburg et al., 2017).

Here we perform an optimum multiparameter (OMP) analysis (Tomczak & Large, 1989) on the long-term hydrographic data from the California Cooperative Oceanic Fisheries Investigations (CalCOFI) program to quantify the spatiotemporal variability of source water contributions to the southern CCS. This water mass history provides context for understanding the drivers and pathways of biogeochemical variability in this region and quantifies regionally heterogeneous impacts driven by oceanic changes occurring far afield.

2. Data and Methods

2.1. Data Sources

We use historical hydrographic data from the World Ocean Database (https://www.nodc.noaa.gov/OC5/WOD/pr_wod.html) and the CalCOFI program (Bograd et al., 2003) in our analyses. Since 1984, CalCOFI has consistently sampled six nominal lines in the southern CCS from San Diego to Pt. Conception quarterly, with target months of January, April, July, and October (Figure 1c), amounting to more than 6,700 station occupations between January 1984 and February 2018. A separate analysis using the CalCOFI data between 1950 and 2018 (over 10,000 station occupations on the modern CalCOFI grid) was also conducted, although prior to 1984 only basic hydrographic variables and dissolved oxygen were routinely measured, so we focus our analysis on 1984 to present. Details of the standard sampling and analysis procedures, along with all data and derived variables, can be found in any of the CalCOFI data reports (e.g., Scripps Institution of Oceanography, 2012) or online at www.calcofi.org.

We define source water masses to the southern CCS with three 10° × 10° boxes centered at 45°N, 135°W; 27°N, 139°W; and 5°N, 108°W, corresponding to Pacific Subarctic Upper Water (PSUW), Eastern North Pacific Central Water (ENPCW), and Pacific Equatorial Water (PEW), respectively (Figure 1a; Tomczak & Godfrey, 2003). PSUW is characterized by relatively low temperature and salinity and high oxygen content, ENPCW is relatively warm and salty near-surface waters, with low nutrient content, and PEW is relatively warm and salty subsurface waters, with relatively high nutrient content (Table S1 in the supporting information). Small variations in the size and location of the source water boxes had little effect on the results (not shown). Available temperature, salinity, dissolved oxygen (DO), phosphate, silicate, and nitrate data within each source water box were extracted from the World Ocean Database 2018 using the WODselect tool (https://www.nodc.noaa.gov/OC5/SELECT/dbsearch/dbsearch.html). Vertical profiles for each variable were obtained from the Ocean Station Data data set and were constrained to those that extended at least 400-m deep and for which each chemical measurement (DO, phosphate, nitrate, and silicate) was accompanied by simultaneous observations of temperature and salinity (Figure 1b and Table S2). For further analysis, each profile was linearly interpolated at 1-m vertical resolution to 1,000 m depth or the maximum depth of the cast. Outliers in the World Ocean Database data were removed by plotting all of the interpolated casts for a given variable and removing any values that exceed two standard deviations at a given depth.

2.2. Optimum Multiparameter Analysis

OMP analysis (Tomczak & Large, 1989) estimates the relative contributions of source water types that mix together to form an observed water mass, assuming that water mass properties are quasi-conservative. An "extended" OMP analysis drops the assumption of conserved tracers in order to account for modification of water masses by remineralization along their advective pathways. In the extended OMP analysis, source water nutrients are set as preformed nutrients (Anderson & Sarmiento, 1994; Brzezinski, 1985; Karstensen & Tomczak, 1998) and deviations from preformed nutrient concentrations are accounted for by the change in phosphate, ΔP (García-Ibáñez et al., 2015; Poole & Tomczak, 1999), which is related to changes in oxygen, nitrate, and silicate through Redfield ratios (Anderson & Sarmiento, 1994; Brzezinski, 1985).

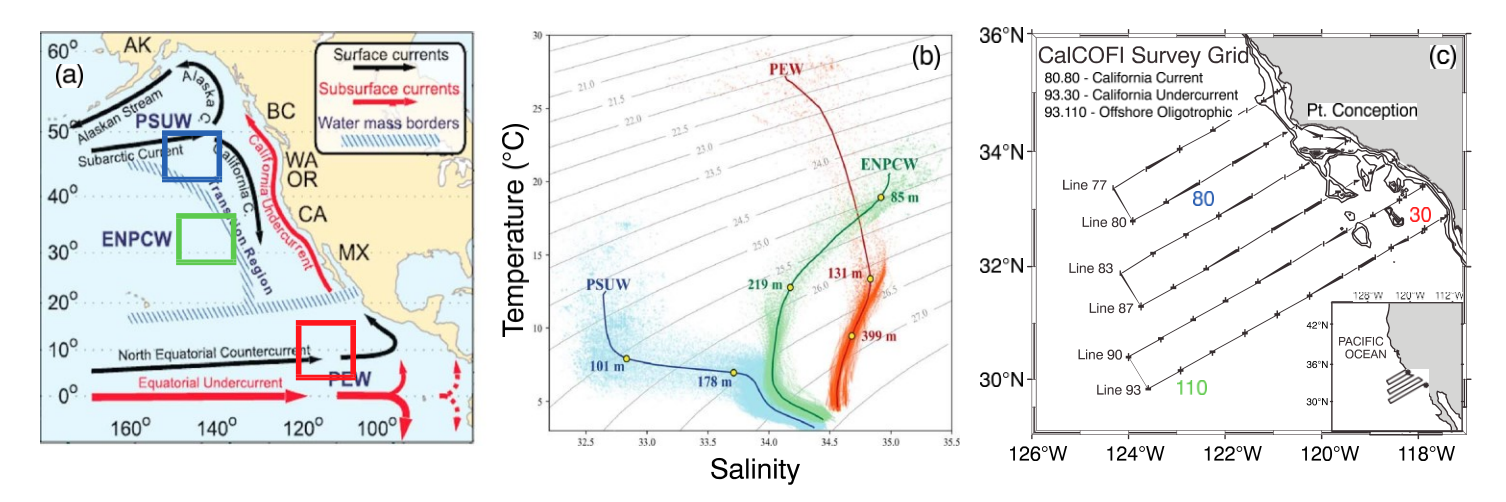


Figure 1. (a) Map of the northeast Pacific showing the source regions for Pacific Subarctic Upper Water (PSUW; blue box), Eastern North Pacific Central Water (ENPCW; green box), and Pacific Equatorial Water (PEW; red box). Map shows dominant surface and subsurface currents in the northeast Pacific, modified from Thomson and Krassovski (2010). (b) Temperature-salinity diagram for PSUW (blue), ENPCW (green), and PEW (red). Data obtained from the World Ocean Database (WOD18) for the period 1984–2017. Marked depth ranges note the upper and lower end-members for each defined water mass. (c) Nominal CalCOFI grid showing Lines and Stations that have been regularly occupied quarterly since 1984. Stations 80.80, 93.30, and 93.110 are labeled.

The first step in OMP analysis is to define the source water characteristics. For each source water region and each parameter, all filtered casts were averaged together to give a mean profile. Upper and lower end-members for each source water type were defined as the end points of linear segments on *T-S* diagrams constructed from the mean temperature and salinity profiles (Figure 1b). Values of each parameter were then extracted for each of six source water end-members (upper and lower PSUW, ENPCW, and PEW; Table S1). With six defined source water masses and six input variables (*T*, *S*, O₂, NO₃, PO₄, and SiO₄), we are left with six equations plus conservation of mass:

$$X_{\text{PEWu}}T_{\text{PEWu}} \trianglerighteq ... \trianglerighteq X_{\text{ENPCWd}}T_{\text{ENPCWd}} \trianglerighteq 0 \frac{1}{4} T_{\text{OBS}} \trianglerighteq R_T$$

$$X_{\text{PEWu}}S_{\text{PEWu}} \trianglerighteq ... \trianglerighteq X_{\text{ENPCWd}}S_{\text{ENPCWd}} \trianglerighteq 0 \frac{1}{4} S_{\text{OBS}} \trianglerighteq R_S$$

$$X_{\text{PEWu}}O_{2;\text{PEWu}} \trianglerighteq ... \trianglerighteq X_{\text{ENPCWd}}O_{2;\text{ENPCWd}} - r_{\text{O=P}} \Delta P \frac{1}{4} O_{2;\text{OBS}} \trianglerighteq R_{\text{O2}}$$

$$X_{\text{PEWu}}PO_{4;\text{PEWu}} \trianglerighteq ... \trianglerighteq X_{\text{ENPCWd}}PO_{4;\text{ENPCWd}} \trianglerighteq \Delta P \frac{1}{4} PO_{4;\text{OBS}} \trianglerighteq R_{\text{PO4}}$$

$$X_{\text{PEWu}}NO_{3;\text{PEWu}} \trianglerighteq ... \trianglerighteq X_{\text{ENPCWd}}NO_{3;\text{ENPCWd}} \trianglerighteq r_{\text{N=P}} \Delta P \frac{1}{4} NO_{3;\text{OBS}} \trianglerighteq R_{\text{NO3}}$$

$$X_{\text{PEWu}}SiO_{4;\text{PEWu}} \trianglerighteq ... \trianglerighteq X_{\text{ENPCWd}}SiO_{4;\text{ENPCWd}} \trianglerighteq r_{\text{Si=P}} \Delta P \frac{1}{4} SiO_{4;\text{OBS}} \trianglerighteq R_{\text{SiO4}}$$

$$X_{\text{PEWu}} \trianglerighteq X_{\text{PSUWu}} \trianglerighteq X_{\text{ENPCWd}} \trianglerighteq X_{\text{PEWd}} \trianglerighteq X_{\text{PSUWd}} \trianglerighteq X_{\text{ENPCWd}} \frac{1}{4} 1 \trianglerighteq R_{\Sigma}$$

where relative source water contributions are denoted by X, Redfield ratios relative to phosphate are denoted by r ($r_{\rm O/P}170$, $r_{\rm N/P}16$, $r_{\rm Si/P}18$), ΔP is the change in phosphate due to remineralization, and R is a residual term. Observations (subscript OBS) are CalCOFI data at each station and depth for the period 1984–2018. Each equation is normalized and weighted using the methods outlined in Tomczak and Large (1989) and the Matlab OMP toolbox (https://www.mathworks.com/matlabcentral/fileexchange/1334-omp-analysis). Following Tomczak and Large (1989), we assigned the mass conservation equation with the same weight as that of the temperature equation. We solve this set of equations minimizing the residuals using a least square method constrained to having nonnegative X and ΔP values.

The equivalent OMP analysis for the longer period (1950–2018) used only three parameters (temperature, salinity, and DO) and three source water end-members (PSUW at 163 m; ENPCWu at 85 m; and PEWd at 399 m, representing the depths of the strongest contributions of each water mass). Select results are presented for comparison in Figure S1, but our focus here is on the 1984 to present period, in which there was consistent sampling of water properties, including inorganic nutrients, over a common grid.

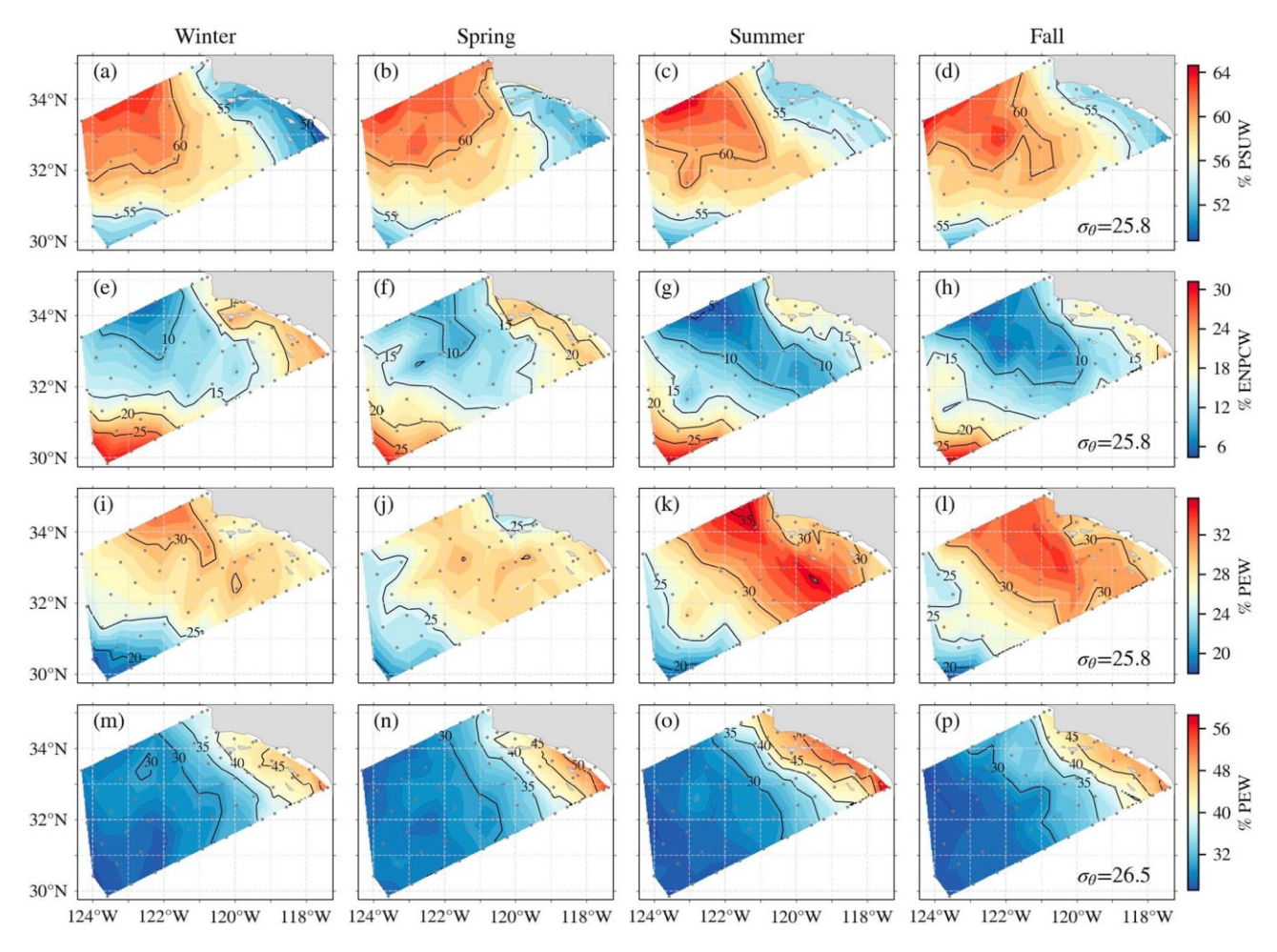


Figure 2. Maps of seasonal mean (1984–2018) water mass contributions for, left to right, winter (January–March), spring (April–June), summer (July–September) and fall (October–November) for (a)–(d) %PSUW on the $\sigma_{\theta} = 25.8 \text{ kg/m}^3$ isopycnal surface, (e)–(h) %ENPCW on the $\sigma_{\theta} = 25.8 \text{ kg/m}^3$ isopycnal surface, and (i)–(l) %PEW on the $\sigma_{\theta} = 25.8 \text{ kg/m}^3$ isopycnal surface, and (m–p) %PEW on the $\sigma_{\theta} = 26.5 \text{ kg/m}^3$ isopycnal surface. PSUW = Pacific Subarctic Upper Water; ENPCW = Eastern North Pacific Central Water; PEW = Pacific Equatorial Water.

We present source water mass contributions in the CalCOFI region in several ways: (i) maps on isopycnal surfaces representing the upper ($\sigma_{\theta} = 25.8 \text{ kg/m}^3$) and lower ($\sigma_{\theta} = 26.5 \text{ kg/m}^3$) pycnocline to highlight changes in source water advection along isopycnals (Bograd et al., 2015), (ii) Hovmöller vertical profiles that reflect both isopycnal displacement and water mass contributions at select stations (Bograd et al., 2015; Figure 1c): Station 80.80 (33°, 28.8'N, 122°, 31.8'W) is located ~220 km offshore of Pt. Conception, typically within the main core of the California Current (Lynn & Simpson, 1987); Station 93.30 (32°, 51.0'N, 117°, 31.8'W) is located over the continental slope within the Southern California Bight (SCB) and is strongly impacted by the California Undercurrent (CUC; Lynn & Simpson, 1987; Lynn & Simpson, 1990); and Station 93.110 (30°, 10.8'N, 122°, 55.2'W) is located more than 600 km offshore of Southern California and represents water masses offshore of the main California Current core, within the oligotrophic North Pacific Subtropical Gyre, and (iii) sections along CalCOFI Line 93 for composite periods representing El Niño (1988, 1992, 1998, and 2016) and La Niña (1989, 1999, 2000, 2008, and 2011) conditions, defined as the winter CalCOFI survey following a strong El Niño or La Niña event.

3. Variability in Water Mass Structure

3.1. Seasonal Means

The contribution of PSUW in the upper waters of the CalCOFI domain reflects the influence of the California Current (Hickey, 1998; Lynn & Simpson, 1987), which advects PSUW into the region from the

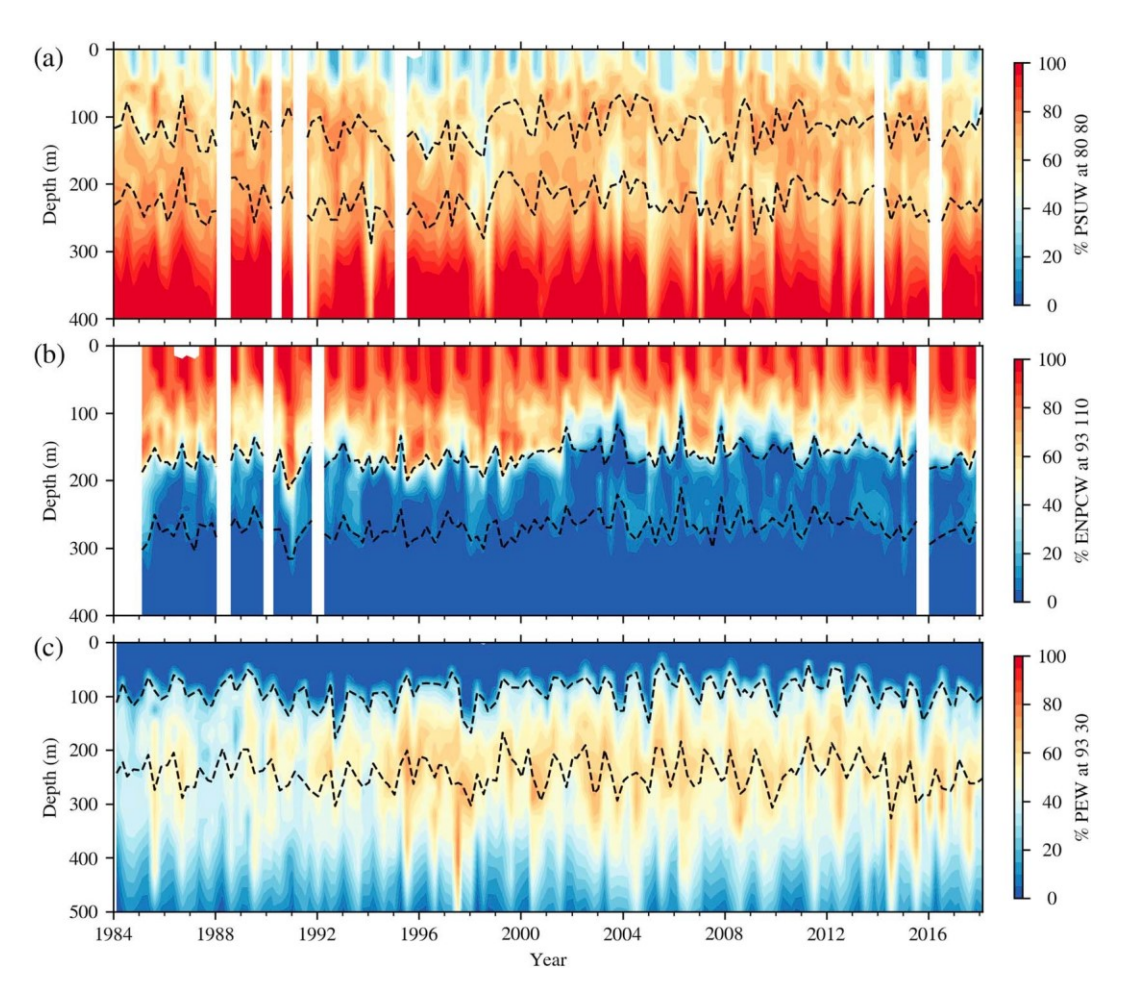


Figure 3. Hovmöller sections of water mass contributions from 1984 to 2018 for (a) %PSUW at Station 80.80 (0–400 m), (b) %ENPCW at Station 93.110 (0–400 m), and (c) %PEW at Station 93.30 (0–500 m). The σ_{θ} = 25.8 kg/m³ and the σ_{θ} = 26.5 kg/m³ isopycnal surfaces are marked on each panel. Data gaps are shown by white bars. PSUW = Pacific Subarctic Upper Water; ENPCW = Eastern North Pacific Central Water; PEW = Pacific Equatorial Water.

north (offshore percentages >60%; Figures 2a–2d), with little seasonal variation. Higher levels of PSUW are found inshore of 122°W off Pt. Conception in spring, reflecting an increase in equatorward transport associated with the transition to upwelling conditions (Lynn et al., 2003). The inshore region has a smaller contribution of PSUW, particularly in winter, and the southern offshore corner of the domain (around Station 93.110) remains limited in PSUW year-round.

A similar spatial pattern is seen in the contribution of relatively warm, high-salinity ENPCW in the upper waters, but with a reversed cross-shore gradient to that of PSUW. Very low percentages (<15%) are found in the core California Current region, higher values inshore, and the highest contribution (>30%) at the southern offshore corner of the domain (Figures 2e–2h). This distribution of ENPCW reflects its source offshore of the region, within the North Pacific Subtropical Gyre, and its intrusion into the domain at the southern offshore corner. The moderately high (20%–25%) contributions within the SCB are likely due to the entrainment of offshore waters within the poleward flowing CUC, and subsequent advection northward (Lynn & Simpson, 1987, 1990). Though this spatial pattern is consistent year round, there is some seasonal variation, with the lowest (highest) contributions of ENPCW in summer-fall (winter-spring).

There is a stronger seasonality in PEW at the shallower surface (σ_{θ} = 25.8 kg/m³), with contributions >30% inshore of the high-PSUW region in summer-fall (Figures 2i–2l). The deeper surface (σ_{θ} = 26.5 kg/m³) within the SCB is dominated by PEW (Figures 2m–2p). The core California Current area west of ~120°W is low in PEW content year round (<30%) and lowest in summer-fall. High values of PEW (>50%) are seen within the SCB and inshore region, reflecting advection of tropical waters within the poleward flowing CUC (Lynn & Simpson, 1987, 1990; Hickey, 1998; Castro et al., 2001; Bograd et al., 2015). This strong cross-shore

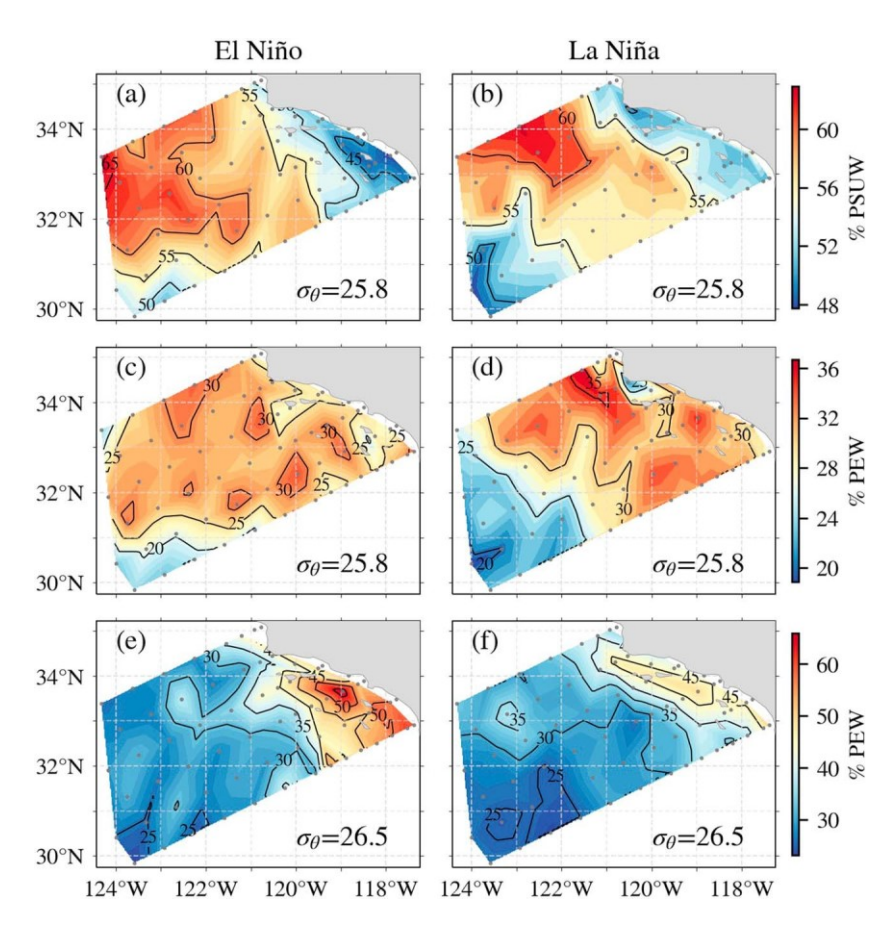


Figure 4. Maps of composite water mass contributions for (left) El Niño and (right) La Niña periods for (a–b) %PSUW on the σ_{θ} = 25.8 kg/m³ isopycnal surface, (c and d) %PEW on the σ_{θ} = 25.8 kg/m³ isopycnal surface, and (e–f) %PEW on the σ_{θ} = 26.5 kg/m³ isopycnal surface. PSUW = Pacific Subarctic Upper Water; PEW = Pacific Equatorial Water.

gradient in lower pycnocline PEW content is seen year-round but is largest in summer, when a stronger CUC likely limits mixing with offshore waters.

3.2. Interannual Variability

Interannual variability in the content and depth structure of the source water masses is evident at stations reflecting the climatological core of the California Current (Station 80.80), the region dominated by intrusion of offshore waters (Station 93.110), and the core of the California Undercurrent (Station 93.30, Bograd et al., 2008, 2015; Figure 3). The primary contribution of PSUW (contributions of 50%–70%) in the upper thermocline occurs around 100–200 m (around $\sigma_{\theta} = 25.8 \text{ kg/m}^3$ at 80.80; Figure 3a), within the California Current core (Lynn & Simpson, 1987), where there is significant interannual variability in both the content and depth profile of PSUW. A weaker and deeper contribution of PSUW is seen during strong El Niño events (e.g., 1998). An apparent strong PSUW contribution at depths greater than 300 m is likely due to limitations of the OMP analysis (see section 4).

At Station 93.110, in the southwest corner of the CalCOFI grid, the highest contribution of ENPCW (>75%) occurs in the upper 150 m, with high variability in its depth profile (Figure 3b). ENPCW content drops off precipitously below the σ_{θ} = 25.8 kg/m³ isopycnal, although smaller concentrations (20%–30%) are seen as deep as 250 to 300 m periodically. There are extended periods of relatively higher (1990–2000) and lower (2002–2012) contributions of ENPCW at this station.

Strong interannual variability in the advection of PEW into the domain is evident at Station 93.30 (Figure 3c). The highest concentration of PEW (60%–80%) is typically found in the lower pycnocline, at depths ranging from \sim 100 m to deeper than 400 m and centered on the σ_{θ} = 26.5 kg/m³ isopycnal, that is,

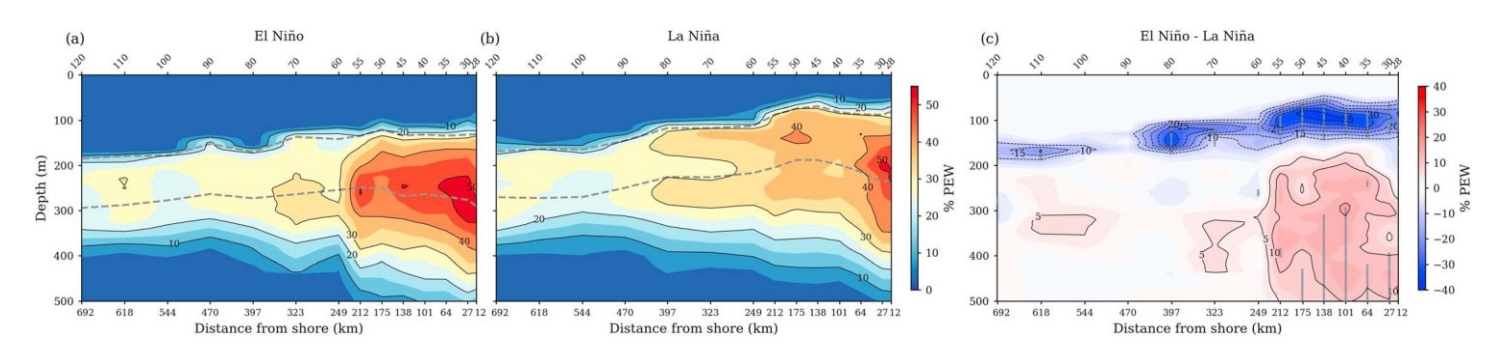


Figure 5. Section along Line 93 of (a) %PEW for the El Niño composite, (b) %PEW for the La Niña composite, and (c) the difference in %PEW between the El Niño and La Niña composites. The $\sigma_{\theta} = 25.8 \text{ kg/m}^3$ and the $\sigma_{\theta} = 26.5 \text{ kg/m}^3$ isopycnal surfaces are marked on (a) and (b). Locations at which the El Niño and La Niña composite mean %PEW is significantly different at p < 0.05 are marked with gray dots in (c). PEW = Pacific Equatorial Water.

within the CUC core (Lynn & Simpson, 1987; Bograd et al., 2015). There is an evident shift to higher PEW content after 1995, with shorter periods of high PEW concentrations during El Niño years (e.g., 1998). This shift to higher PEW concentration corresponds to, and reflects, the observed trends in subsurface concentrations of oxygen (declining) and inorganic nutrient (increasing) content in this part of the CalCOFI domain (Bograd et al., 2008, 2015) and supports the hypothesis of a stronger CUC and larger influence of tropical waters in recent years (Meinvielle & Johnson, 2013; Bograd et al., 2015; McClatchie et al., 2018). The three-member OMP performed over the full CalCOFI period, 1950–2018, shows similar patterns to the post-1984 period (Figure S1), although large temporal gaps preclude identification of trends.

The time series plots reveal that the ENSO cycle affects source water contributions to the southern CCS (Figure 3). In the upper thermocline, El Niño periods are characterized by higher concentrations of PSUW offshore, but lower PSUW content within the SCB as compared to La Niña periods (Figures 4a and 4b). As expected, there is higher PEW content inshore on the deeper isopycnal during El Niño events (>50% compared to ~40% during La Niña events; Figures 4e and 4f), reflecting a strengthened CUC (Gómez-Valdivia et al., 2017; Lynn & Bograd, 2002). However, the pattern of increased PEW during El Niño does not hold for the upper thermocline, which reflects not only the deep PEW source but also its interaction with upwelling that is typically stronger during La Niña than during El Niño. While these differences illustrate qualitative CCS responses to ENSO, they reach statistical significance in only a few places owing to a relatively small sample size and the loose coupling of the CCS to ENSO when viewed on an event scale (e.g., Fiedler & Mantua, 2017).

The relative contribution of PEW during El Niño and La Niña events is more clearly seen in the composite PEW sections along Line 93 (Figure 5). The higher contribution of PEW is evident during El Niño periods, reflecting stronger advection from the south in the CUC; however, these waters are distributed deeper in the water column and farther offshore than they are during La Niña periods. The difference section reveals an up to 30% enhancement of PEW during La Niña in the upper 150 m, with this effect extending more than 200 km offshore (Figure 5c). Thus, even though there is a stronger PEW signature in the CUC during El Niño events, there is a higher content of PEW in the upper water column during La Niña events. The stronger upwelling and deeper upwelling source depths seen during La Niña events (M. G. Jacox et al., 2015) supply more PEW to the euphotic zone, providing a biological pathway for La Niña to impact the near surface expression of source waters, including increased potential for amplification of hypoxic and low pH events (Nam et al., 2011).

4. Discussion and Conclusions

The relative contributions of subarctic (PSUW), subtropical (ENPCW), and tropical (PEW) source waters to the southern CCS reveal substantial heterogeneity in water mass structure. Spatially, there is a strong subsurface cross-shore gradient from PEW dominance in the SCB and coastal regions up to Pt. Conception to PSUW dominance in the offshore region. These patterns reflect the advective pathways of these water masses, within the California Current in the upper 200 m for PSUW and within the California Undercurrent at 200–300 m for PEW. ENPCW is a relatively weak contributor to water masses in this

8



region, primarily impacting the southwest corner of the domain and, to a lesser extent, the SCB and coastal regions following recirculation and entrainment within the poleward CUC flow. Although the seasonal variability of this water mass structure is weak along isopycnals representing the main advective pathways, strong interannual variability is evident, impacting both the magnitude and water column distribution of the source water masses. In particular, changes in upwelling strength and the depth distribution of PEW over the ENSO cycle allow for these nutrient-rich waters to be more effectively tapped by primary producers during La Niña events. We caution that this heterogeneity in water mass structure reduces the efficacy of using spatial averages to describe temporal variability in the southern CCS, as they can mask the importance of independent variations in source waters.

There are limitations to our OMP analysis. Results are dependent on the choice of source water end-members, although a sensitivity study using different source regions and end-member depths did not significantly change the results (not shown). Nonetheless, our selected source water end-members are most efficiently tuned for waters in the upper and lower pycnocline in the CalCOFI domain, where historical biogeochemical trends have been observed (Bograd et al., 2008, 2015). Highest values of the ΔP term, which attributes changes in phosphate content (and subsequently the other nonconservative tracers through the Redfield ratio) to water mass transformation along the advective pathways, occur at depths greater than 300 m, that is, below the primary influence of both the California Current and CUC (Figure S2). Similarly, the residuals from the OMP analysis, while small, are greatest in the surface layer, whose ephemeral nature is not expected to retain source water properties, and the deepest layers (400-500 m), which are not as well represented by the source water masses and for which water mass transformations may have occurred (Figures S2 and 3). Further refinement of the source water end-members could reduce these residuals, although our analysis has provided a valuable description of the varying water mass structure in the southern CCS. Future work will focus on the predictive capacity and biological implications of this source water variability, which can inform strategies for adapting management to anticipated climate-induced ecosystem disruptions.

Acknowledgments

World Ocean Database data are available at https://www.nodc.noaa. gov/OC5/SELECT/dbsearch/dbsearch. html CalCOFI data are available at http://www.calcofi.org. The Matlab OMP toolbox is available at https:// www.mathworks.com/matlabcentral/ fileexchange/1334-omp-analysis. We acknowledge the quality and longevity of the CalCOFI program, and the many scientists and seagoing staff who have contributed to the collection, processing, and analysis of this excellent data set. We also acknowledge the California Current Ecosystem Long-Term Ecosystem Research (CCE-LTER) project, supported by a grant from NSF (OCE-0417616). We thank two anonymous reviewers for helpful comments on a previous draft. S. J. B. conceived the project with input from IDS and MGJ, I. D. S. performed the OMP analysis, and S. J. B. wrote the paper with contributions from IDS and MGJ.

References

- Anderson, L. A., & Sarmiento, J. L. (1994). Redfield ratios of remineralization determined by nutrient data analysis. Global Biogeochemical Cycles, 8(1), 65–80. https://doi.org/10.1029/93GB03318
- Andrews, O. D., Buitenhuis, E., Le Quere, C., & Suntharalingam, P. (2017). Biogeochemical modeling of dissolved oxygen in a changing ocean. Philosophical Transactions of the Royal Society A, 375(2102), 20160328. https://doi.org/10.1098/rsta.2016.0328
- Bograd, S. J., Buil, M. P., Lorenzo, E. D., Castro, C. G., Schroeder, I. D., Goericke, R., et al. (2015). Changes in source waters to the Southern California Bight. *Deep Sea Research Part II: Topical Studies in Oceanography*, 112, 42–52. https://doi.org.10.1016/j. dsr2.2014.04.009
- Bograd, S. J., Castro, C. G., Di Lorenzo, E., Palacios, D. M., Bailey, H., Gilly, W., & Chavez, F. P. (2008). Oxygen declines and the shoaling of the hypoxic boundary in the California current. *Geophysical Research Letters*, 35, L12607. https://doi.org/10.1029/
- Bograd, S. J., Checkley, D. M., & Wooster, W. S. (2003). CalCOFI: a half century of physical, chemical, and biological research in the California current system. *Deep-Sea Research Part II*, 50(14–16), 2349–2353. https://doi.org/10.1016/S0967-0645(03)00122-X
- Bopp, L., Resplandy, L., Untersee, A., Le Mezo, P., & Kageyama, M. (2017). Ocean (de)oxygenation from the Last Glacial Maximum to the twenty-first century: Insights from Earth System models. *Philosophical Transactions of the Royal Society A*, 375(2102), 20160323. https://doi.org/10.1098/rsta.2016.0323
- Breitburg, D., Levin, L. A., Oschlies, A., Grégoire, M., Chavez, F. P., Conley, D. J., et al. (2018). Declining oxygen in the global ocean and coastal waters. *Science*, 359(6371), eaam7240. https://doi.org/10.1126/science.aam7240
- Brzezinski, M. A. (1985). The Si:C:N ratio of marine diatoms: Interspecific variability and the effect of some environmental variables 1. Journal of Phycology, 21(3), 347–357.
- Castro, C. G., Chavez, F. P., & Collins, C. A. (2001). Role of the California Undercurrent in the export of denitrified waters from the eastern tropical North Pacific. Global Biogeochemical Cycles, 15(4), 819–830. https://doi.org/10.1029/2000GB001324
- Chan, F., Barth, J. A., Lubchenco, J., Kirincich, A., Weeks, H., Peterson, W. T., & Menge, B. A. (2008). Emergence of anoxia in the California current large marine ecosystem. *Science*, 319(5865), 920. https://doi.org/10.1126/science.1149016
- Deutsch, C., Brix, H., Ito, T., Frenzel, H., & Thompson, L. (2011). Climate-forced variability of ocean hypoxia. *Science*, 333(6040), 336–339. https://doi.org/10.1126/science.1202422
- Deutsch, C., Emerson, S., & Thompson, L. (2005). Fingerprints of climate change in North Pacific oxygen. *Geophysical Research Letters*, 32, L16604. https://doi.org/10.1029/2005GL023190
- Doney, S. C., Fabry, V. J., Feely, R. A., & Kleypas, J. A. (2009). Ocean acidification: the other CO₂ problem. *Annual Review of Marine Science*, 1(1), 169–192. https://doi.org/10.1146/annurev.marine.010908.163834
- Fiedler, P. C., & Mantua, N. J. (2017). How are warm and cool years in the California Current related to ENSO? *Journal of Geophysical Research: Oceans*, 122, 5936–5951. https://doi.org/10.1002/2017]C013094
- García-Ibáñez, M. I., Pardo, P. C., Carracedo, L. I., Mercier, H., Lherminier, P., Rios, A. F., & Perez, F. F. (2015). Structure, transports and transformations of the water masses in the Atlantic Subpolar Gyre. Progress in Oceanography, 135, 18–36. https://doi.org/10.1016/j.pocean.2015.03.009



- Gómez-Valdivia, F., Parés-Sierra, A., & Laura Flores-Morales, A. (2017). Semiannual variability of the California Undercurrent along the Southern California Current System: A tropical generated phenomenon. *Journal of Geophysical Research: Oceans*, 122, 1574–1589. https://doi.org/10.1002/2016JC012350
- Gruber, N. (2011). Warming up, turning sour losing breath: Ocean biogeochemistry under global change. *Philosophical Transactions of the Royal Society A*, 369(1943), 1980–1996. https://doi.org/10.1098/rsta.2011.0003
- Gruber, N., Hauri, C., Lachkar, Z., Loher, D., Frolicher, T. L., & Plattner, G.-K. (2012). Rapid progression of ocean acidification in the California Current. Science, 337(6091), 220–223. https://doi.org/10.1126/science.1216773
- Hauri, C., Gruber, N., Plattner, G.-K., Alin, S., Feely, R. A., Hales, B., & Wheeler, P. A. (2009). Ocean acidification in the California Current System. *Oceanography*, 22(4), 60–71. https://doi.org/10.5670/oceanog.2009.97
- Hickey, B. A. (1998). Western North America, tip of Baja California to Vancouver Island. In K. Brink & A. Robinson (Eds.), The Sea, vol. 11 (pp. 345–394). New York: Wiley.
- Huyer, A. (2003). Preface to special section on enhanced subarctic influence in the California Current, 2002. *Geophysical Research Letters*, 30(15), 8019. https://doi.org/10.1029/2003GL017724
- Jacox, M., Bograd, S. J., Hazen, E. L., & Fiechter, J. (2015). Sensitivity of the California Current nutrient supply to wind, heat, and remote ocean forcing. Geophysical Research Letters, 42, 5950–5957. https://doi.org/10.1002/2015GL065147
- Jacox, M. G., Fiechter, J., Moore, A. M., & Edwards, C. A. (2015). ENSO and the California Current coastal upwelling response. *Journal of Geophysical Research: Oceans*, 120, 1691–1702. https://doi.org/10.1002/2014JC010650
- Karstensen, J., & Tomczak, M. (1998). Age determination of mixed water masses using CFC and oxygen data. *Journal of Geophysical Research*, 103(C9), 18,599–18,609. https://doi.org/10.1029/98JC00889
- Keeling, R. F., Kortzinger, A., & Gruber, N. (2010). Ocean deoxygenation in a warming world. Annual Review of Marine Science, 2(1), 199–229. https://doi.org/10.1146/annurev.marine.010908.163855
- Koslow, J. A., Davison, P., Ferrer, E., Jimenez-Rosenberg, S. P. A., Aceves-Medina, G., & Watson, W. (2018). The evolving response of mesopelagic fishes to declining midwater oxygen concentrations in the southern and central California Current. *ICES Journal of Marine Science*, fsy154. https://doi.org/10.1093/icesjms/fsy154
- Levin, L. (2018). Manifestation, drivers, and emergence of open ocean deoxygenation. Annual Review of Marine Science, 10(1), 229–260. https://doi.org/10.1146/annurev-marine-121916-063359
- Limburg, K. E., Breitburg, D., & Levin, L. A. (2017). Ocean deoxygenation—A climate-related problem. Frontiers in Ecology and the Environment, 15(9). https://doi.org/10.1002/fee.1728
- Lynn, R. J., & Bograd, S. J. (2002). Dynamic evolution of the 1997-1998 El Niño-La Niña cycle in the southern California Current System. Progress in Oceanography, 54(1-4), 59-75. https://doi.org/10.1016/S0079-6611(02)00043-5
- Lynn, R. J., Bograd, S. J., Chereskin, T. K., & Huyer, A. (2003). Seasonal renewal of the California current: The spring transition off California. *Journal of Geophysical Research*, 108(C8), 3279. https://doi.org/10.1029/2003JC001787
- Lynn, R. J., & Simpson, J. J. (1987). The California current system: the seasonal variability of its seasonal characteristics. *Journal of Geophysical Research*, 92(C12), 12,947–12,966. https://doi.org/10.1029/JC092iC12p12947
- Lynn, R. J., & Simpson, J. J. (1990). The flow of the Undercurrent over the continental borderland off southern California. Journal of Geophysical Research, 95(C8), 12,995–13,008. https://doi.org/10.1029/JC095iC08p12995
- McClatchie, S., Gao, J., Drenkard, L., Thompson, A., Watson, W., Ciannelli, L., et al. (2018). Interannual and secular variability of mesopelagic and forage fishes in the southern California Current System. *Journal of Geophysical Research: Oceans*, 123(9), 6277–6295. https://doi.org/10.1029/2018JC014011
- McClatchie, S., Goericke, R., Cosgrove, R., Auad, G., & Vetter, R. (2010). Oxygen in the Southern California Bight: Multidecadal trends and implications for demersal fisheries. *Geophysical Research Letters*, 37, L19602. https://doi.org/10.1029/2010GL044497
- Meinvielle, M., & Johnson, G. C. (2013). Decadal water-property trends in the California Undercurrent, with implications for ocean acidification. *Journal of Geophysical Research: Oceans*, 118, 6687–6703. https://doi.org/10.1002/2013JC009299
- Nam, S., Kim, H.-J., & Send, U. (2011). Amplification of hypoxic and acidic events by La Niña conditions on the continental shelf off California. Geophysical Research Letters, 38, 1.22602. https://doi.org/10.1029/2011GL049549
- Nam, S., Takeshita, Y., Frieder, C. A., Martz, T., & Ballard, J. (2015). Seasonal advection of Pacific Equatorial Water alters oxygen and pH in the Southern California Bight. *Journal of Geophysical Research: Oceans*, 120, 5387–5399. https://doi.org/10.1002/2015JC010859
- Poole, R., & Tomczak, M. (1999). Optimum multiparameter analysis of the water mass structure in the Atlantic Ocean thermocline. *Deep-Sea Research Part II*, 46(11), 1895–1921. https://doi.org/10.1016/S0967-0637(99)00025-4
- Schmidtko, S., Stramma, L., & Visbeck, M. (2017). Decline in global oceanic oxygen content during the past five decades. *Nature*, 542(7641), 335–339. https://doi.org/10.1038/nature21399
- Schroeder, I. D., Santora, J. A., Bograd, S. J., Hazen, E. L., Sakuma, K. M., Moore, A. M., et al. (2018). Source water variability as a driver of rockfish recruitment in the California Current Ecosystem: Implications for climate change and fisheries management. *Canadian Journal of Fisheries and Aquatic Sciences*, 1–11. https://doi.org/10.1139/cjfas-2017-0480
- Scripps Institution of Oceanography (SIO). (2012). Data report, CalCOFI cruise 1110. CC Ref. 12-05, La Jolla, CA, 59 pp.
- Stramma, L., Johnson, G. C., Sprintall, J., & Mohrholz, V. (2008). Expanding oxygen-minimum zones in the tropical oceans. *Science*, 320(5876), 655–658. https://doi.org/10.1126/science.1153847
- Stramma, L., Schmidtko, S., Levin, L. A., & Johnson, G. C. (2010). Ocean oxygen minima expansions and their biological impacts. *Deep-Sea Research Part I*, 57, 1–9.
- Thomson, R. E., & Krassovski, M. V. (2010). Poleward reach of the California Undercurrent extension. *Journal of Geophysical Research*, 115(C9), C09027. https://doi.org/10.1029/2010|C006280
- Tomczak, M., & Godfrey, J. S. (2003). Regional oceanography: An introduction, (2nd ed.p. 390). Delhi: Daya Publishing House.
- Tomczak, M., & Large, D. G. B. (1989). Optimum multiparameter analysis of mixing in the thermocline of the eastern Indian Ocean. *Journal of Geophysical Research*, 94(C11), 16,141–16,149. https://doi.org/10.1029/JC094iC11p16141
- Watanabe, Y. W., Shigemitsu, M., & Tadokoro, K. (2008). Evidence of a change in oceanic fixed nitrogen with decadal climate change in the North Pacific subpolar region. Geophysical Research Letters, 35, L01602. https://doi.org/10.1029/2007GL032188
- Whitney, F. A., Bograd, S. J., & Ono, T. (2013). Nutrient enrichment of the subarctic Pacific Ocean pycnocline. *Geophysical Research Letters*, 40, 2200–2205. https://doi.org/10.1002/grl.50439
- Whitney, F. A., Freeland, H. J., & Robert, M. (2007). Persistently declining oxygen levels in the interior waters of the eastern subarctic Pacific. *Progress in Oceanography*, 75(2), 179–199. https://doi.org/10.1016/j.pocean.2007.08.007